JACS
JOURNAL OF THE AMERICAN CHEMICAL SOCIETY

Article

pubs.acs.org/JACS

Selective Detection and Inhibition of Active Caspase-3 in Cells with Optimized Peptides

Chris J. Vickers, Gonzalo E. González-Páez, and Dennis W. Wolan*

Departments of Molecular and Experimental Medicine and Chemical Physiology, The Scripps Research Institute, 10550 North Torrey Pines Road, La Jolla, California 92037, United States

Supporting Information

ABSTRACT: Caspases are a family of cysteine-aspartyl proteases that are well recognized for their essential roles in apoptosis and inflammation. Recently, caspases have also been linked to the promotion of other biologically important phenomena, such as cellular differentiation and proliferation. Dysregulation of the multifaceted and indispensable activities of caspases has been globally linked to several diseases, including cancer and neurodegenerative disorders; however, the specific caspase members responsible for these diseases have yet to be assigned. Activity-based probes (ABPs) and peptide-based inhibitors are instrumental in the detection and control of protease activity and serve as alternative methods to genetic approaches. Such molecules aid in the interrogation of specific proteases within cellular and animal models as well as help elucidate aberrant proteolytic function correlated to disease phenotypes. No ABPs or inhibitors have been discovered that specifically target one of the eleven human caspases in a cellular context. Therefore, ascribing distinct contributions to an individual caspase activity within naturally occurring biological systems is not possible. Herein, we describe a peptide series optimized for the selective detection and inhibition of active caspase-3 in cells. These compounds exhibit low nanomolar potency against caspase-3 with >120-fold selectivity over caspase-7 which shares 77% active site identity. Our ability to individually target wild-type active caspase-3 for detection and cell permeable inhibition is a valuable proof-of-concept methodology that can be readily employed to probe the significance of caspase-3 in apoptosis, neurological disorders, cardiovascular diseases, and sepsis.

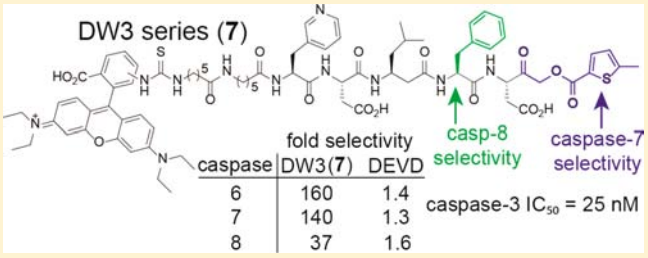

INTRODUCTION

Human caspases encompass a family of eleven cysteine-aspartyl proteases that are essential for the initiation (caspases-2, -8, -9, and -10) and execution (caspases-3, -6, and -7) of apoptosis,[1,2] cytokine activation and inflammation (caspases-1, -4, and -5),[3,4] and epidermal differentiation (caspase-14).[5−8] Aside from these well-documented functions, several of these caspases have been linked to a variety of other cellular processes, including proliferation and survival.[9,10] As with most proteases, caspases are synthesized and stored as inactive zymogens, or procaspases, and are tightly regulated by several upstream mechanisms until their activity is required.[11−16] Despite these relatively fail-safe pathways, dysregulation of caspase function can drive the propagation of several diseases. For example, the inability to activate apoptotic-related procaspases can result in tumorigenesis,[17,18] whereas uncontrolled activity of the same subset of caspases is implicated in neurodegenerative disorders,[19−21] cardiovascular disease,[22−24] and sepsis.[25,26]

Caspase-3 is the most well-studied member of this family and is critical for carrying out the final steps of cellular dismantling during apoptosis as well as the differentiation of neuronal and skeletal muscle cells. Homodimeric procaspase-3 is processed into the mature enzyme by upstream proteases (caspases-2, -6, -8, -9, and -10) or self-activation that cleaves the protein into large (p20) and small (p12) subunits.[11−16] Subsequent removal of the N-terminal prodomain converts the large subunit into the fully processed p17 domain and results in the fully active caspase-3 heterotetramer.[11−16] Due to the correlation of caspase-3 activity with cellular destruction, the protease has been targeted for the development of small molecule activators to incite cell death irrespective of any aberrant oncogenic proteins upstream of caspase-3 maturation.[27,28] Conversely, caspase-3 is a target for chemical and/or biological inhibitors as a means to prevent neurodegenerative disorders, such as Huntington's disease where caspase-3 hydrolyzes the mutant huntingtin (mhtt) protein that leads to neuronal toxicity.[20]

The cellular consequences of caspase-3 activity, together with the highly homologous caspase-7, are well annotated, and several biochemical and cell-based methods have begun to tackle the difficult task of resolving the individual substrates and contributions that these caspases have within both healthy and disease states.[29,30] To this end, genetic engineering applications such as RNAi,[31,32] gene knockout,[33] and cell lines with orthogonally activated caspase mutants[34,35] have provided valuable insight into caspase-3 function and the effects of gene silencing on cellular biological responses. However, these laborious techniques have several significant drawbacks,

Received: June 24, 2013
Published: August 5, 2013

   dx.doi.org/10.1021/ja406399r | J. Am. Chem. Soc. 2013, 135, 12869−12876

including insufficient knockdown of protein levels, low-throughput, and difficulty in the manufacture and validation of artificial conditions. Activity-based probes (ABPs) provide an alternative method to these genetic approaches to not only inhibit caspase-3 activity but also specifically detect the mature protease within a cellular environment. ABPs are commonly employed as high-throughput, nonintrusive, and easily accessible methods for the study of protease function in cell-based and in vivo biological models.[36−40] Protease-directed ABPs typically contain three structural features: (1) a N-terminal tag (e.g., biotin) or label (e.g., fluorophore) for the enrichment or visualization of the probe, respectively; (2) a peptide recognition sequence for binding to the protease (usually a tetrapeptide for caspases); and (3) a C-terminal electrophilic warhead for the covalent attachment of the ABP to the active site nucleophilic residue. For the caspase active site cysteine thiol, such warheads include aldehydes, epoxides, halomethyl ketones, Michael acceptors, and acyloxymethyl ketones (AOMKs). In addition, innovative work using fluorophore/quencher pairs have enabled the spatial and temporal visualization of general caspase activity in living cells.[41,42] Unfortunately, no ABPs have been designed that are selective for a particular endogenous caspase isoform.[43] Commercially available ABPs used to study caspase-3 activity are based on the DEVD peptide recognition sequence historically derived from positional-scanning combinatorial libraries (PSCLs).[44] This work laid the foundation for caspase-specific substrates, inhibitors, and ABPs; however, these compounds have promiscuous activity within the caspase family. For example, DEVD recognizes caspases-3, -6, -7, and -8, and inhibitors based on this sequence (**1**) inhibit these enzymes with nearly the same efficacy (Figure 1A).

To advance our understanding of caspase biology and elucidate the roles each caspase isoform has during the progression of disease and other biologically important phenomena, we report the optimization and characterization of an ABP that has high potency and specificity for caspase-3. We also describe a cell-permeable inhibitor that is >120-fold selective for caspase-3 over the highly homologous caspase-7 which shares >77% active site sequence identity.

METHODS AND MATERIALS

Caspase Expression and Purification. Caspases-3, -6, -7, and -8 were expressed and purified as previously described.[28,45]

Chemical Synthesis and Purification. Compounds **1**−**9** were synthesized based on procedures from Kato et al. using solid-phase peptide synthesis.[40] **1**−**8** were attached to 2-chlorotrityl chloride resin (2-ClTrCl) solid support (EMD Millipore) via the carboxylic acid side chain of the P1 Asp residue (Figure 2), while **9** was linked to solid support through hydrazone formation with the ketone moiety as previously described.[40] Unnatural amino acids Fmoc-3 Pal−OH and Fmoc-β-homoLeucine−OH (PepTech), rhodamine B isothiocyanate (Rho) (Santa Cruz), and 5(6)-carboxyfluorescein (FAM) (AnaSpec) were used as received from suppliers. After synthesis, each compound was subsequently purified by reverse-phase preparative-HPLC (Hitachi) using a C18 column and prepared as 10 mM DMSO stock solutions.

IC_{50} Determination. Inhibitor, recombinant caspase, and substrate [Ac-DEVD-AFC: caspases-3/7, Ac-VEID-AFC: caspase-6, and Ac-IETD-AFC: caspase-8] were all diluted into an assay buffer consisting of 50 mM HEPES pH 7.4, 0.1% CHAPS, 10 mM KCl, 50 mM sucrose, 1 mM $MgCl_2$, and 10 mM DTT. An amount of 20 μL of diluted inhibitor (2.5 ×) and 20 μL of (2.5 ×) caspase solution [final concentrations: 10 nM caspase-3, 50 nM caspase-6, 10 nM caspase-7, or 25 nM caspase-8] was added to NUNC 96-well, black, low-binding,

A

	N-terminal cap	recognition sequence	C-terminal warhead	IC_{50} values (nM) casp-3	casp-6	casp-7	casp-8
1	FAM-	DEVD-	AOMK	18	26	24	29
2	FAM-Ahx_2-	CV3-	AOMK	27	3000	1300	100
3	Acetyl-	CV3-	AOMK	23	3400	730	400
4	Acetyl-	CV3-	KE	6.8	>10000	730	190
5	Acetyl- F-D-ßhLeu-hLeu-D-		KE	12	>5000	650	210
6	Acetyl-	DW3-	KE	16	>10000	1900	920
7	Rho-Ahx_2-	DW3-	KE	25	4000	3500	930
8	Rho-	DEVD-	AOMK	10	65	17	12

B

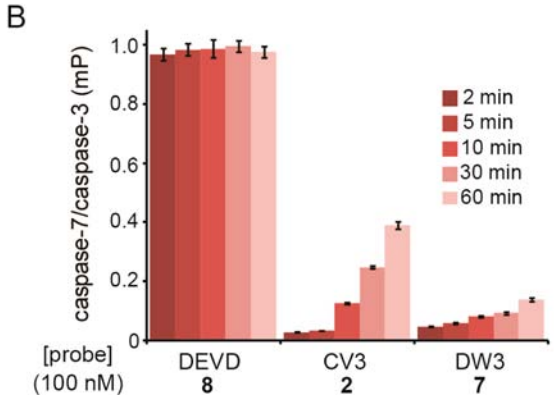

Figure 1. In vitro selectivity of CV3 and DW3 series ABPs and inhibitors for caspase-3. (A) Compound IC_{50} values against recombinant caspases as measured by turnover of fluorogenic substrate. (B) Fluorescence polarization comparison of DEVD (**8**), CV3 (**2**), and DW3 (**7**) ABPs for binding caspase-3 or -7 measured after 2, 5, 10, 30, or 60 min of incubation. Both probes and caspases were used at 100 nM final concentrations.

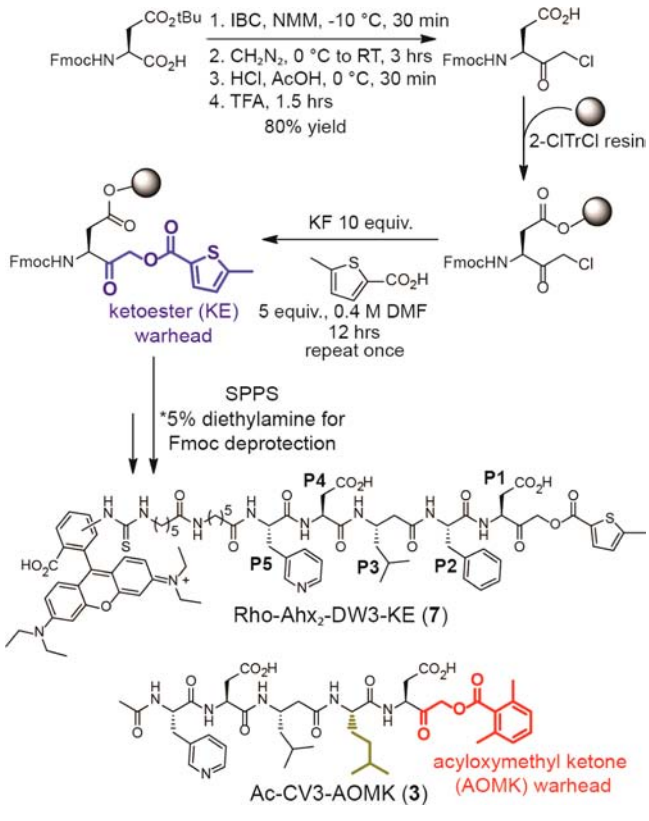

Figure 2. Synthesis of caspase-3 selective ABPs and inhibitors.

dx.doi.org/10.1021/ja406399r | J. Am. Chem. Soc. 2013, 135, 12869−12876

microtiter plates. This solution was incubated for 2 min at room temperature followed by a 10 μL (5 ×) addition of the corresponding caspase substrate to a final concentration of 50 μM. The initial rate of substrate turnover (RFU/s) was then immediately analyzed on a PerkinElmer EnVision plate reader with excitation at 355 nm and emission detection at 486 nm. At least three replicates were included for each data set, which was analyzed using GraphPad Prism to calculate the corresponding IC_{50} values.

FP Assay. Caspases and ABPs were diluted into an assay buffer consisting of 50 mM HEPES pH 7.4, 0.1% CHAPS, 10 mM KCl, 50 mM sucrose, 1 mM $MgCl_2$, and 10 mM DTT. An amount of 25 μL of (2 ×) recombinant caspase-3 or -7 (100 nM final concentration) was added to NUNC 96-well, black, low-binding, microtiter plates, followed by 25 μL of (2 ×) Rho-DEVD-AOMK (**8**), FAM-Ahx_2-CV3-AOMK (**2**), or Rho-Ahx_2-DW3-KE (**7**) (100 nM final concentration). This solution was incubated at room temperature for the indicated time periods before the FP was read on a PerkinElmer EnVision plate reader with excitation at 480 nm and emission detection at 535 nm. ΔmP values are normalized by subtraction of control wells with probe only.

Cellular Viability Assays. HeLa, U-87 MG, MDA-MB-231, NCI-H460, HL-60, HT-29, and MCF-7 cells were cultured as described by the ATCC using 10% FBS and Pen/Strep/Glutamine at 37 °C with 5% CO_2. Cells were plated into sterile 96-well tissue culture-treated plates to a total volume of 50 μL at a density of 5000 cells/well 12 h prior to each experiment. An amount of 25 μL of 3× staurosporine (STS) (LC Laboratories) or media containing the vehicle DMSO (0.5% final concentration) was subsequently added and incubated with cells for indicated time periods. An amount of 75 μL of CellTiter-Glo reagent (Promega) was then added to assess cell viability followed by shaking for 10 min at RT. An amount of 100 μL of solution from each well was then transferred into NUNC 96-well, white, low-binding, microtiter plates, and luminescence was measured on a PerkinElmer EnVision plate reader.

Caspase Labeling with ABPs in Cell Lysate. Cells were grown to ∼80% confluency in 150 mm dishes before addition of control media (0.5% DMSO), STS (1 or 5 μM), or superFasL (150 ng/mL) (Enzo Life Sciences). Cells were incubated with reagents for indicated time periods prior to being gently scrapped from the dish surface. Cells were pelleted at 1000 rpm and washed twice with cold PBS before lysis in an assay buffer (50 mM HEPES pH 7.4, 0.1% CHAPS, 10 mM KCl, 50 mM sucrose, 1 mM $MgCl_2$, and 10 mM DTT) by Dounce homogenization. Lysates were then clarified by centrifugation for 30 min at 4 °C and 14 000 rpm. Supernatants were incubated with fluorescent ABPs for indicated time periods and probe concentrations with all aliquots subjected to standardization for total protein concentration with a BCA assay. Samples were subsequently quenched with reducing LDS sample loading buffer containing SDS and boiled for 5 min. After SDS-PAGE, gels were visualized for fluorescence using a Typhoon flat bed scanner. Western blotting with GAPDH antibody (Cell Signaling) was used as a loading control.

Caspase Visualization in Nuclear and Cytoplasmic Extract. HeLa nuclear and cytoplasmic cellular extracts were separated with the NE-PER* Nuclear and Cytoplasmic Extraction Kit (Thermo). As an adjustment to the extraction protocol, for every 250 μL of cell pellet, 1.25 mL of CER1 reagent, 60 μL of CER2 reagent, and 150 μL of NER reagent were used for each extraction. Prior to lysis, cells were washed twice with cold PBS. Before labeling with ABPs, extracts were diluted 2-fold with caspase assay buffer (50 mM HEPES pH 7.4, 10 mM KCl, 50 mM sucrose, 1 mM $MgCl_2$, and 10 mM DTT). ABP (200 nM final concentration) was then incubated with each sample for 1 h prior to quenching with reducing LDS sample loading buffer containing SDS with boiling for 5 min. Extracts were subjected to Western blot and probed with α-tubulin and PARP antibodies (Cell Signaling) as controls for cytoplasmic and nuclear extract purity, respectively.

Caspase-3 Inhibition Using Cell-Permeable Peptides. Ac-DW3(OMe)-KE (**9**) or Z-VAD-FMK (LC Laboratories) was preincubated at 75 μM with HeLa cells for 5 h followed by addition of STS to a final concentration of 1 μM for indicated time periods. Cells were then washed twice with cold PBS, harvested, and labeled with ABPs as described by Dounce homogenization.

RESULTS AND DISCUSSION

Optimization and In Vitro Characterization of Caspase-3 Selective Compounds. We recently identified and characterized a peptide-based ABP/inhibitor CV3 series (**2** and **3**, respectively) with >30-fold caspase-3 selectivity over caspase-7 via incorporation of several unnatural amino acids into the canonical DEVD tetrapeptide (Figure 1).[46] Two of the key substitutions that boost specificity include exchange of the P3 Glu with a β-homoleucine (βhLeu) and the addition of 3-pyridylalanine (3 Pal) as an extra amino acid at the N-terminus P5 position (Figure 1). We sought to improve caspase-3 selectivity, as significant off-target labeling of caspase-7 was observed with this first generation CV3 series ABP (**2**) upon labeling STS-induced apoptotic cell lysates. Moreover, our original CV3 ABP (**2**) had <4-fold selectivity against active caspase-8 (Figure 1A).

To improve our caspase-3-specific compounds and reduce off-target interactions with caspases-7 and -8, we initially focused on optimization of the commonly employed 2,6-dimethylbenzoic acid-derived ester group (AOMK) C-terminal warhead (Figures 1 and 2). We began with the synthesis of Ac-DEVD-AOMK (**S1**) as a control and showed the peptide inhibitor is highly promiscuous as evidenced by the small IC_{50} ratios for caspase-6, -7, and -8 over caspase-3 which were 10, 1.0, and 2.0, respectively (Figure S1, Supporting Information). We subsequently synthesized a library of Ac-DEVD-X peptides where X is replaced by a set of 24 unique warhead derivatives (Figure S1, Supporting Information). As derivatization of the prime side chemical leaving groups of caspase-directed ABPs is not well reported within the literature, we investigated a diverse range of functional groups, steric hindrances, and electronics to identify a warhead with improved selectivity for caspase-3 (Figure S1, Supporting Information). In addition, we hypothesized that the selectivity of a unique prime side warhead would synergistically improve caspase-3 specificity when combined with a nonprime side caspase-3-directed peptide such as our CV3 series sequence (Figure 2). We identified several warheads with appreciable tunable and selective effects against particular caspase isoforms (Figure S1, Supporting Information). Notable examples include a 4-phenylbenzoate ester warhead (**S4**) that provides 60-fold selectivity for caspase-3 over caspase-6 with DEVD as the peptide sequence; an additional 4-fold selectivity for caspase-3 over caspase-7 was achieved using a 5-methyl-2-thiophene carboxylic acid-derived warhead (**S13**); and a 7-fold selectivity for caspase-3 over caspase-8 was obtained using a cinchophen-derived warhead (**S6**) (Figure S1, Supporting Information). For improved discrimination against caspase-7, we moved forward with the 5-methyl-2-thiophene carboxylate-derived ketoester group, which we termed "KE" (Figures 1 and 2).

The new KE warhead appended onto our original CV3 peptide (**4**) resulted in 110-fold and 28-fold selectivity for caspase-3 over caspases-7 and -8, respectively (Figure 1A). On the basis of our X-ray crystal structures of caspases-3, -7, and -8 in complex with CV3, the P5 pyridine side chain makes a potential hydrogen bond with the side chain of N261 in caspase-8 but has no interaction with caspases-3 or -7.[46] To abrogate this interaction and gain more selectivity for caspase-3 over caspase-8, we replaced the P5 3 Pal of CV3 with Phe (**5**) (Figure 1A). Surprisingly, this substitution reduced the

dx.doi.org/10.1021/ja406399r | J. Am. Chem. Soc. 2013, 135, 12869−12876

selectivity between caspase-3 and -7 by 2-fold and 1.5-fold against caspase-8, suggesting the Phe-containing inhibitor (**5**) may bind the caspase active site in an alternate conformation relative to CV3 (Figure 1A). Also based on our crystal structures, we determined the CV3 P2 homoleucine (hLeu) residue has a minimal influence on selectivity among caspases-3 and -7, as the hydrophobic pocket formed by the two proteases that orients the peptide chain is nearly identical (caspase-3: W206, F256, Y204; caspase-7: W232, F282, Y230).[46] However, we could exploit selectivity against caspase-8 at the P2 position as the corresponding residues in caspase-8 (Y412, N458, V410) have reduced propensity for π-stacking.[46] We therefore replaced the P2 hLeu in our CV3 series with Phe in our DW3 series (**6**, **7**) (Figures 1 and 2). This substitution resulted in two improved features over the CV3 series, including: (1) an increased selectivity of the DW3 series for caspase-3 against both caspases-7 and -8 and (2) replacement of the extraneous P2 unnatural amino acid for Phe significantly reduces the cost and improves the ease and accessibility of synthesis (Figures 1 and 2). Our Ac-DW3-KE (**6**) inhibitor has 120-fold selectivity for caspase-3 compared to caspase-7 and 58-fold selectivity against caspase-8 (Figure 1A). The corresponding second-generation DW3 ABP Rho-Ahx$_2$-DW3-KE (**7**) has 140- and 37-fold selectivity for caspase-3 over caspases-7 and -8, respectively (Figure 1A). For comparison, we synthesized the corresponding ABP with an N-terminal rhodamine fluorophore appended onto the canonical DEVD tetrapeptide (Rho-DEVD-AOMK, **8**) and found <2-fold selectivity between caspases-3, -7, and -8 (Figure 1A). We have previously found that addition of 6-aminohexanoic acid (Ahx) linkers between the fluorophore and the peptide recognition sequence slightly improves caspase-3 selectivity over caspase-7.[46]

We employed the fluorophore-containing ABPs of the DEVD (**8**), CV3 (**2**), and DW3 (**7**) series of compounds to compare the selectivity and binding kinetics as measured by fluorescence polarization (FP) (Figure 1B). Here, 100 nM of each probe was incubated with physiologically relevant concentrations of caspase-3 or -7 (100 nM).[47,48] FP was measured at 2, 5, 10, 30, and 60 min for interaction between the caspase and ABP (Figure 1B). The fluorophore-tagged ABPs undergo increased polarization upon binding to the much larger caspase protein with a concomitant increase in millipolarizations (mP) (Figure 1B). Caspases-3 and -7 bind rapidly to Rho-DEVD-AOMK (**8**) and obtain nearly identical maximum levels of ΔmP (Figure 1B). Our first generation probe FAM-Ahx$_2$-CV3-AOMK (**2**) interacts more rapidly with caspase-3 compared to caspase-7. However, after 60 min of incubation, caspase-7 eventually binds the covalent probe as evidenced by the ∼40% FP relative to caspase-3 binding (Figure 1B). Our new Rho-Ahx$_2$-DW3-KE (**7**) provides a combination of rapid and robust binding to caspase-3 with slow and discriminate interaction with caspase-7 (Figure 1B). Importantly, despite the covalent and irreversible properties of the probe, Rho-Ahx$_2$-DW3-KE (**7**) has <15% of the FP when incubated with caspase-7 compared to caspase-3 even after 60 min of reaction time (Figure 1B).

Specific Caspase-3 Labeling in Cellular Lysates. We further evaluated whether the in vitro caspase-3-directed specificity of **7** would translate into a cellular system where the intrinsic inducer STS was used to activate apoptosis-associated caspases (Figure 3). HeLa cells were incubated with 1 μM STS for 6 h followed by cell lysis and addition of varying concentrations of either **8** or **7** (1000, 200, 40, or 8 nM final concentrations) for 15 min or with a 200 nM probe for varying time periods (2, 15, 30, 60, 180, or 360 min) (Figure 3). Rho-DEVD-AOMK (**8**) promiscuously labeled the large subunits that contain the active site cysteine of caspase-3 (p17/20), caspase-6 (p19), and caspase-7 (p22) at all probe concentrations and incubation periods tested (Figure 3A). In comparison, Rho-Ahx$_2$-DW3-KE (**7**) only detected the p20 and p17 subunits of active caspase-3 (Figure 3B). Importantly, no background labeling of active caspase-7 is observed after incubation of the apoptotic lysate with large excesses of **7** (1 μM) for 15 min (Figure 3B). Furthermore, procaspase-3, which

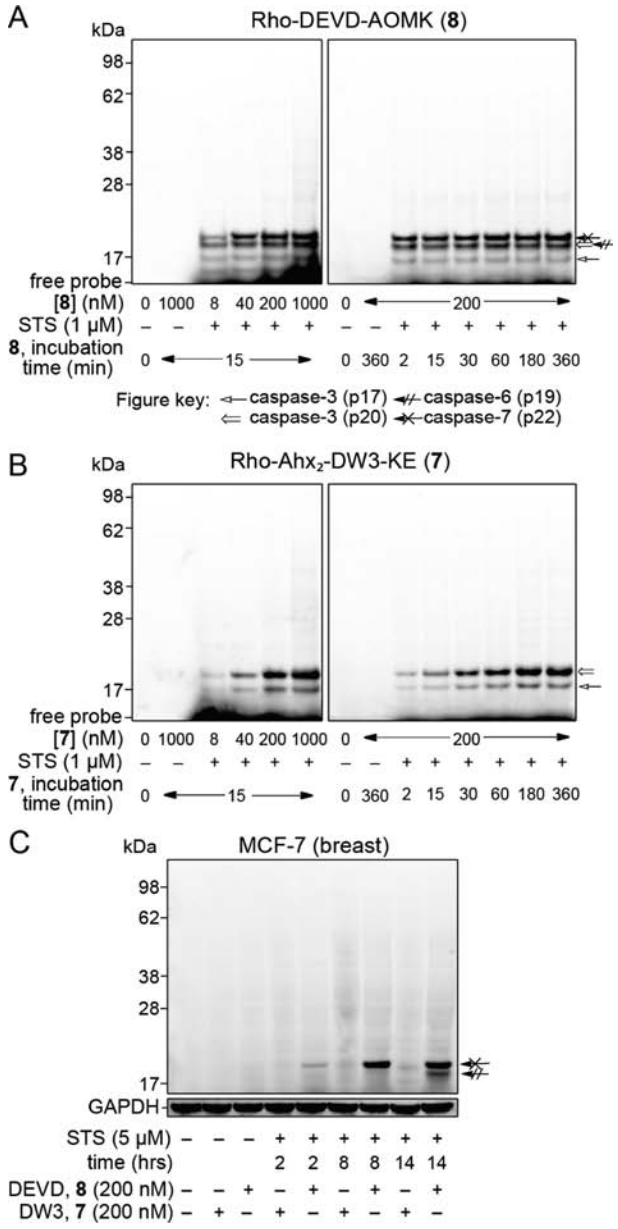

Figure 3. Cell lysate labeling with our caspase-3-specific ABP **7**. (A) Nonspecific labeling of executioner caspases with a rhodamine-containing ABP based on the canonical DEVD recognition tetrapeptide (Rho-DEVD-AOMK (**8**)) in STS-induced apoptotic lysates. (B) Rho-Ahx$_2$-DW3-KE (**7**) does not label caspase-7 (p22) or any other proteins despite application of large excesses of probe and extended incubation times. (C) Caspase labeling in apoptotic MCF-7 cell lysates induced using 5 μM STS with samples taken at 2, 8, and 14 h.

dx.doi.org/10.1021/ja406399r | J. Am. Chem. Soc. 2013, 135, 12869−12876

lacks internal cleavage between the large and small subunits and a properly formed active site for binding peptide-based probes, remained undetected as well as any other off-target proteins (Figure 3B).

To further verify that **7** is specific for caspase-3 and not active caspases-6 or -7, we used MCF-7 cells that lack a functional caspase-3 protein and monitored active caspase production with **7** or **8** over 14 h of 5 μM STS-induced apoptosis (Figure 3C).[49,50] At 8 and 14 h post STS treatment, an intense band for caspase-7 and a slight band for caspase-6 could be observed using the general ABP Rho-DEVD-AOMK (**8**) (Figure 3C). In contrast, Rho-Ahx$_2$-DW3-KE (**7**) did not label either active caspase-6 or -7 (Figure 3C). A key result from the MCF-7 analysis includes the discrimination of Rho-Ahx$_2$-DW3-KE (**7**) against caspase-6 binding as we can now accurately assess the caspase-3 p20/p17 ratio (+ and − the N-terminal 28 residue prodomain) for all other cell lines that express a functional caspase-3. This comparison is not possible with DEVD-based probes using SDS-PAGE as the caspase-3 p20 and caspase-6 p19 bands are irresolvable and therefore can be contaminated with unknown levels of active caspase-6. This improvement in specific caspase-3 detection and resolution now provides the ability to study the role of the prodomain in caspase biology, which a multitude of evidence suggests is important for cellular localization and scaffolding.[51,52]

Rho-Ahx$_2$-DW3-KE (**7**) was next employed to visualize the kinetics of caspase-3 activation in a variety of cancer cell lines undergoing intrinsic or extrinsic apoptosis induced with 1 μM STS or 150 ng/mL of superFasL, respectively (Figure 4A–C). Each cell line and apoptotic condition was monitored over a 14 h time course at 2 h intervals for cell viability and activated caspases (Figure 4A). Rho-DEVD-AOMK (**8**) indiscriminately labeled the executioner caspases in each cell line and condition that was tested; however, only caspase-3 was covalently targeted by Rho-Ahx$_2$-DW3-KE (**7**) (Figure 4B,C). Interestingly, the ratio of p20/p17 varied dramatically among the different cell lines employed in the study. HeLa lysates had the highest p20/p17 ratio, whereas U-87 MG, HL-60, and NCI-H460 cells generate lower p20/p17 ratios over the course of intrinsic STS-induced apoptosis (Figure 4B). MDA-MB-231 and HT-29 cells activated comparable ratios of p20/p17 over the 14 h experiment (Figure 4B).

In comparison to the measured cell viability data, we were unable to correlate the active caspase-3 p20/p17 ratio with susceptibility to STS-induced apoptosis among the cell lines studied (Figure 4A,B). However, early caspase-3 induction is associated with an increase in kinetics and magnitude of apoptosis as HL-60 cells are the most sensitive to STS treatment and robust levels of active caspase-3 are detected after 2 h with Rho-Ahx$_2$-DW3-KE (**7**) (Figure 4A,B). Extrinsically induced cell death of HeLa with superFasL generated a significant amount of active caspase-3 at the early time points as assessed by Rho-Ahx$_2$-DW3-KE (**7**). Surprisingly, despite the relatively high level of active caspase-3 at the 2 and 4 h time points, a much slower decrease in overall cell viability was measured in comparison to the STS-induced cells (Figure 4A–C). These results suggest that a multitude of other factors govern the rate and extent of cell death aside from intracellular amounts of active caspase-3.

We next sought to apply our ABPs to monitor caspase-3 subcellular localization and improve the spatial resolution of activated caspase-3. Apoptosis studies based on various cell lines, cell death inducers, and immunodetection techniques

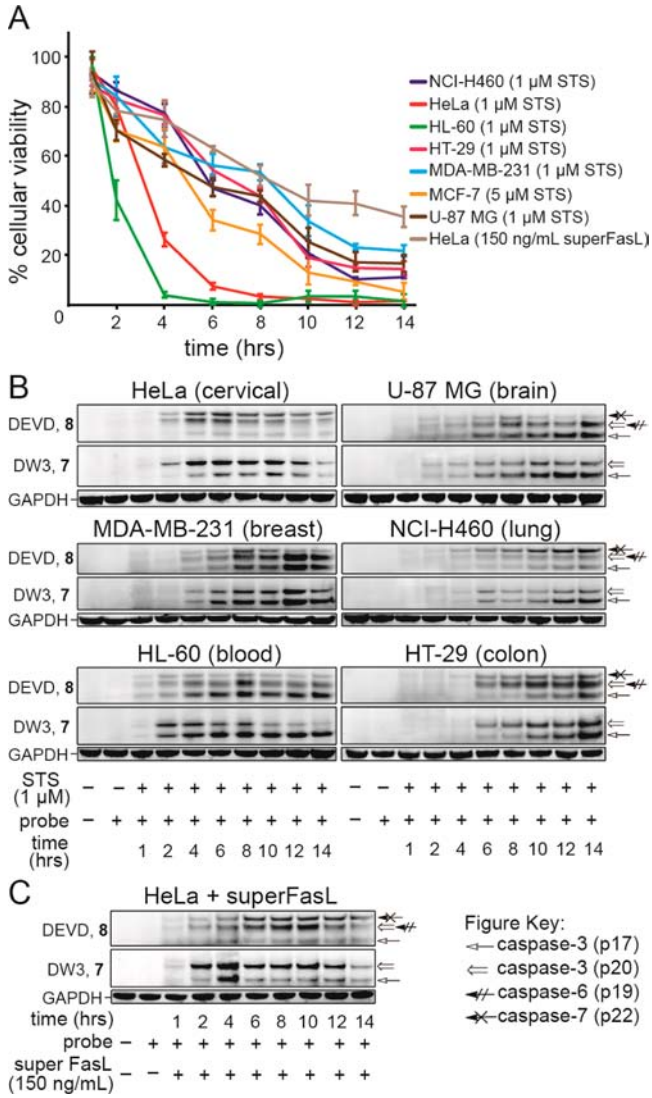

Figure 4. Versatility of **7** for specifically labeling caspase-3 in lysates from a diverse array of cell lines. (A) Rate of cell death as assessed by cellular viability measurements at 1, 2, 4, 6, 8, 10, 12, and 14 h post treatment with indicated apoptotic inducer. (B) ABPs **7** and **8** specifically label caspase-3 and general executioner caspases, respectively, in a variety of cell lines. (C) Extent of caspase activation measured by **7** and **8** in extracts of HeLa cells induced by the extrinsic inducer superFasL (150 ng/mL).

have resulted in conflicting reports as to the nuclear translocation properties of mature caspase-3.[53,54] To address the ability of caspase-3 to be detected in the nucleus with our ABP, cytoplasmic and nuclear fractions of HeLa cells undergoing intrinsic apoptosis were separated and incubated with Rho-DEVD-AOMK (**8**) or Rho-Ahx$_2$-DW3-KE (**7**) for 60 min, separated by SDS-PAGE, and visualized for fluorescence. Active caspase-3 was detected by **7** and **8** in both nuclear and cytoplasmic extracts after 2 h of incubation with 1 μM STS (Figure 5).

Our ABP **7** bound appreciably higher levels of active caspase-3 p17 in both cytoplasmic and nuclear fractions of HeLa cells relative to **8** (Figure 5). Moreover, active caspase-3 disappears more rapidly over 12 h within the cytoplasm (Figure 5). Importantly, we can exploit the Rho-Ahx$_2$-DW3-KE (**7**) caspase-3 selective properties to assess the fraction of active caspase-3 that retains the N-terminal prodomain sequence

dx.doi.org/10.1021/ja406399r | J. Am. Chem. Soc. 2013, 135, 12869–12876

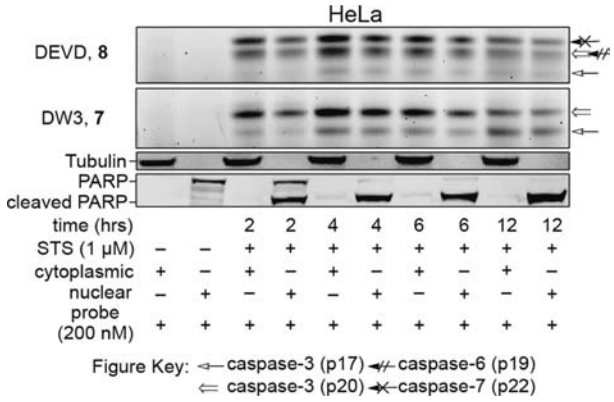

Figure 5. Caspase detection in HeLa cell cytoplasmic and nuclear extracts upon apoptosis induction with 1 μM STS. Cells were harvested at 2, 4, 6, and 12 h of STS incubation followed by separation of cytoplasmic and nuclear fractions and incubation with either **8** or **7** (200 nM) for 60 min. α-Tubulin and PARP antibodies were used to assess the purity of cytoplasmic and nuclear fractions, respectively.

(p20) in the nuclear fraction relative to the fully mature p17 large domain, supporting previous proposals that the prodomain directs cellular localization (Figure 5).[52] The prodomain of caspase-2 has been shown to guide the nuclear localization, and additional cellular studies with caspase-3-specific ABPs will help elucidate the prodomain nuclear translocation properties.[52]

Active Caspase-3 Inhibition in Intact Cells. To further broaden the applicability of our caspase-3-specific molecules, we made a cell-permeable inhibitor version of **6** for selective abrogation of active caspase-3 in live cells (Ac-DW3(OMe)-KE, **9**) (Figure 6A). This inhibitor includes methyl esters in place of the P4 and P1 carboxylic acids which neutralize the negative charge on the molecule and must be removed by esterases for activity against caspase-3.[12,55] Inhibition of protein function with small molecules is a more convenient approach than biochemical methods such as RNAi, knockout models, and engineered proteins as these methods are labor intensive and based on genetically modified systems. Currently, these methods are the only option for selective inhibition or removal of individual caspase family members from cellular environments. A previously reported state-of-the-art anilinoquinazoline inhibitor series was identified to be ~40-fold selective for caspase-3 versus caspase-7 using recombinant enzymes; however, this level of selectivity is not sufficient to abrogate off-target reactivity with caspase-7 in cellular systems.[46,56] This is best evidenced by the complete elimination of DEVDase activity in apoptotic cells attributable to the silencing of both caspase-3 and -7 upon addition of the compounds.[56] These inhibitors also suffer from ~100-fold less potency than our newly identified compound series.[56]

We compared **9** with the commercially available caspase inhibitor Z-VAD-FMK which is known to promiscuously inhibit all executioner caspase function.[57] We preincubated **9** or Z-VAD-FMK at a final concentration of 75 μM with HeLa cells for 5 h prior to addition of 1 μM STS. Cells were subjected to cellular viability studies and detection of active caspases at 2, 4, 6, and 8 h post STS (Figure 6B–D). In the absence of either caspase peptide inhibitors (DMSO vehicle only), robust caspase activation can be observed upon incubation of lysates with ABPs **7** and **8** (Figure 6B,C). Preincubation of HeLa cells with Z-VAD-FMK significantly

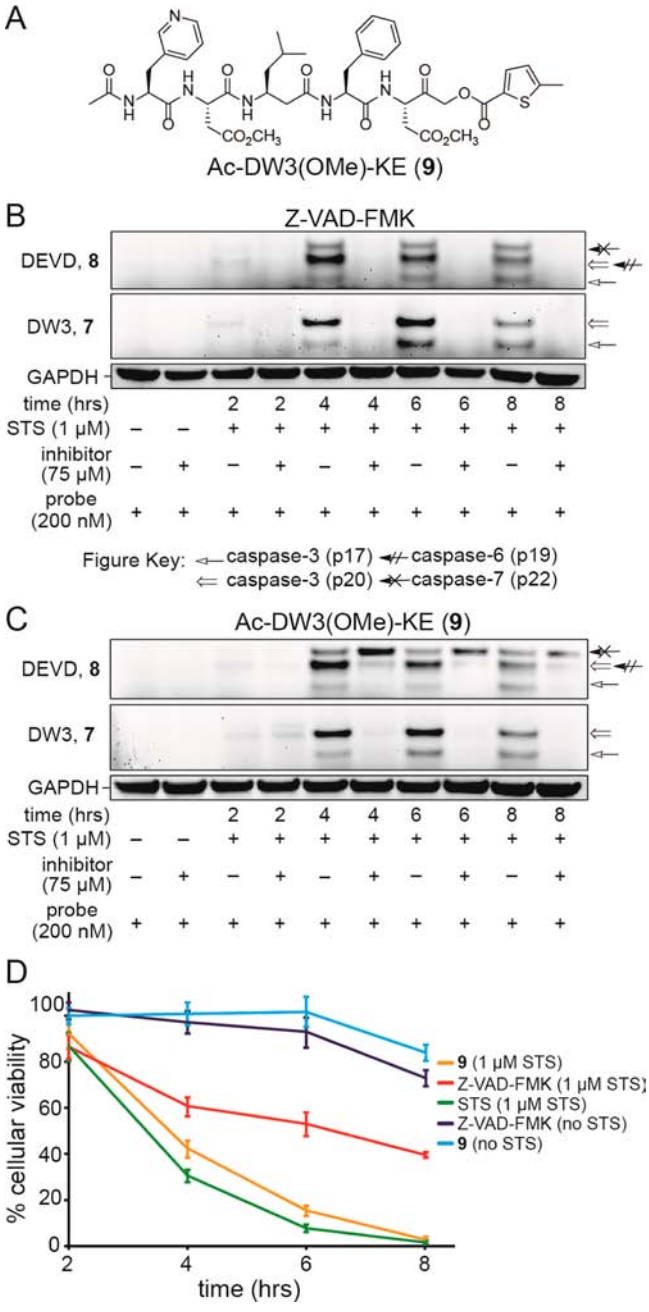

Figure 6. Characterization of the cell-permeable caspase-3 inhibitor Ac-DW3(OMe)-KE (**9**). (A) Chemical structure of **9** with esterified carboxylic acids for increased cell penetration. Visualization of caspase activity in HeLa cells using **8** or **7** (200 nM) after preincubation for 5 h with either Z-VAD-FMK (B) or **9** (C) at 75 μM and incubation with 1 μM STS for 5 h. Z-VAD-FMK blocks all caspase activity, while **9** selectively inhibits caspase-3. (D) Comparison of Z-VAD-FMK and **9** (75 μM) in toxicity and apoptosis protection assays using HeLa cells. Cells were preincubated with inhibitor for 5 h prior to addition of STS.

blocks initiator and executioner caspase activity, resulting in no observable caspase active site labeling with the ABPs (Figure 6B). In comparison, Ac-DW3(OMe)-KE (**9**) significantly reduces the amount of active caspase-3 (p20/p17) labeling without interference from caspase-7 (p22) (Figure 6C). In the presence of Ac-DW3(OMe)-KE (**9**), a considerable increase in active caspase-7 detection occurs, suggesting that the hydrolytic activity of upstream proteases focuses on processing

dx.doi.org/10.1021/ja406399r | J. Am. Chem. Soc. 2013, 135, 12869–12876

procaspase-7 or that the elimination of active caspase-3 promotes interaction of **8** with caspase-7 (Figure 6C).[46]

We next sought to determine if preincubation with **9** or Z-VAD-FMK protects HeLa cells from STS-induced apoptosis. Inhibitors **9** and Z-VAD-FMK were introduced into HeLa cell cultures 5 h prior to addition of STS and were subsequently assessed for viability at 2, 4, 6, and 8 h (Figure 6D). Importantly, both compounds exhibit minimal toxicity at 75 μM in the absence of STS treatment (Figure 6D). Only incubation with Z-VAD-FMK significantly protected HeLa cells from STS-induced apoptosis (Figure 6D). Pretreatment with Ac-DW3(OMe)-KE (**9**) resulted in minimal ability to protect HeLa cells from STS (Figure 6D). These results suggest several likely scenarios, including (1) low concentrations of caspase-3 escape inhibition by **9** and sufficiently induce apoptosis, or (2) active caspases-6 and -7 are capable of rapid cellular dismantling of HeLa cells during apoptosis (Figure 6D).

CONCLUSIONS

The ability to selectively detect and inhibit individual caspase family members in cellular environments provides crucial advantages over genetic approaches that can be utilized in the study of caspase-related diseases and other biological processes. To this end, we report the optimization and characterization of a series of peptide-based ABPs and inhibitors that incorporate a unique warhead and unnatural amino acids with selective affinity toward active caspase-3. Importantly, we show that these molecules can be applied to examine the spatial and temporal resolution of caspase-3 maturation during apoptosis. This technology provides an unparalleled foundation that can now be applied to specifically monitor and characterize caspase-3 activity during disease progression (e.g., cancer and neurodegenerative disorders) as well as to help shed light on the biological role of caspase-3 during cell differentiation and proliferation. The specific substrates and functions of individual caspases are largely unknown due to the close homology and overlapping substrate specificities among members of the caspase family, and specific chemical detection and regulation of individual caspases has yet to be achieved. By incorporating key unnatural amino acids and optimizing the ketoester warhead, we have identified an ABP/inhibitor series that will help advance our understanding of caspase biology.

ASSOCIATED CONTENT

Supporting Information

New compound characterization as well as Figure S1. This material is available free of charge via the Internet at http://pubs.acs.org.

AUTHOR INFORMATION

Corresponding Author

wolan@scripps.edu

Notes

The authors declare no competing financial interest.

ACKNOWLEDGMENTS

We thank Profs. Benjamin Cravatt, Hugh Rosen, Reza Ghadiri, and Jim Paulson for instrumentation. We also gratefully acknowledge financial support from The Scripps Research Institute and the National Science Foundation (predoctoral fellowship to C.J.V.).

REFERENCES

(1) Riedl, J. R.; Shi, Y. *Nat. Rev. Mol. Cell Biol.* **2004**, *5*, 897.
(2) Fuchs, Y.; Steller, H. *Cell* **2011**, *147*, 742.
(3) Martin, S. J.; Henry, C. M.; Cullen, S. P. *Mol. Cell* **2012**, *46*, 387.
(4) Strowig, T.; Henao-Mejia, J.; Elinav, E.; Flavell, R. *Nature* **2012**, *481*, 278.
(5) Fernando, P.; Kelly, J. F.; Balazsi, K.; Slack, R. S.; Megeney, L. A. *Proc. Natl. Acad. Sci. U.S.A.* **2002**, *99*, 11025.
(6) Fujita, J.; Crane, A. M.; Souza, M. K.; Dejosez, M.; Kyba, M.; Flavell, R. A.; Thomson, J. A.; Zwaka, T. P *Cell Stem Cell* **2008**, *2*, 595.
(7) Larsen, B. D.; Rampalli, S.; Burns, L. E.; Brunette, S.; Dilworth, F. J.; Megeney, L. A. *Proc. Natl. Acad. Sci. U.S.A.* **2010**, *107*, 4230.
(8) Basu, S.; Rajakaruna, S.; Menko, A. S. *J. Biol. Chem.* **2012**, *287*, 8384.
(9) Lamkanfi, M.; Festjens, N.; Declercq, W.; Vanden Berghe, T.; Vandenabeele, P. *Cell Death Differ.* **2007**, *14*, 44.
(10) Kikuchi, M.; Kuroki, S.; Kayama, M.; Sakaguchi, S.; Lee, K. K.; Yonehara, S. *J. Biol. Chem.* **2012**, *287*, 41165.
(11) Boatright, K. M.; Salvesen, G. S. *Curr. Opin. Cell Biol.* **2003**, *15*, 725.
(12) Pop, C.; Salvesen, G. S. *J. Biol. Chem.* **2009**, *284*, 21777.
(13) Salvesen, G. S.; Dixit, V. M. *Proc. Natl. Acad. Sci. U.S.A.* **1999**, *96*, 10964.
(14) Shi, Y. *Cell* **2004**, *117*, 855.
(15) Feeney, B.; Clark, A. C. *J. Biol. Chem.* **2005**, *280*, 39772.
(16) Keller, N.; Grütter, M. G.; Zerbe, O. *Cell Death Differ.* **2010**, *17*, 710.
(17) Devarajan, E.; Sahin, A. A.; Chen, J. S.; Krishnamurthy, R. R.; Aggarwal, N.; Brun, A. M.; Sapino, A.; Zhang, F.; Sharma, D.; Yang, X. H.; Tora, A. D.; Mehta, K. *Oncogene* **2002**, *21*, 8843.
(18) Olsson, M.; Zhivotovsky, B. *Cell Death Differ.* **2011**, *18*, 1441.
(19) Graham, R. K.; Deng, Y.; Slow, E. J.; Haigh, B.; Bissada, N.; Lu, G.; Pearson, J.; Shehadeh, J.; Bertram, L.; Murphy, Z.; Warby, S. C.; Doty, C. N.; Roy, S.; Wellington, C. L.; Leavitt, B. R.; Raymond, L. A.; Nicholson, D. W.; Hayden, M. R. *Cell* **2006**, *125*, 1179.
(20) Leyva, M. J.; Degiacomo, F.; Kaltenbach, L. S.; Holcomb, J.; Zhang, N.; Gafni, J.; Park, H.; Lo, D. C.; Salvesen, G. S.; Ellerby, L. M.; Ellman, J. A. *Chem. Biol.* **2010**, *17*, 1189.
(21) D'Amelio, M.; Sheng, M.; Cecconi, F. *Trends Neurosci.* **2012**, *35*, 700.
(22) Communal, C.; Sumandea, M.; de Tombe, P.; Narula, J.; Solaro, R. J.; Hajjar, R. J. *Proc. Natl. Acad. Sci. U.S.A.* **2002**, *99*, 6252.
(23) Cai, L.; Li, W.; Wang, G.; Guo, L.; Jiang, Y.; Kang, Y. J. *Diabetes* **2002**, *51*, 1938.
(24) Moretti, A.; Weig, H. −J.; Ott, T.; Seyfarth, M.; Holthoff, H. −P.; Grewe, D.; Gillitzer, A.; Bott-Flügel, L.; Schömig, A.; Ungerer, M.; Laugwitz, K. −L. *Proc. Natl. Acad. Sci. U.S.A.* **2002**, *99*, 11860.
(25) Hotchkiss, R. S.; Chang, K. C.; Swanson, P. E.; Tinsley, K. W.; Hui, J. J.; Klender, P.; Xanthoudakis, S.; Roy, S.; Black, C.; Grimm, E.; Aspiotis, R.; Han, Y.; Nicholson, D. W.; Karl, I. E. *Nat. Immunol.* **2000**, *1*, 496.
(26) Hotchkiss, R. S.; Nicholson, D. W. *Nat. Rev. Immunol.* **2006**, *6*, 813.
(27) Putt, K. S.; Chen, G. W.; Pearson, J. M.; Sandhorst, J. S.; Hoagland, M. S.; Kwon, J. −T.; Jin, H.; Churchwell, M. I.; Cho, M. −H.; Doerge, D. R.; Helferich, W. G.; Hergenrother, P. J. *Nat. Chem. Biol.* **2006**, *2*, 543.
(28) Wolan, D. W.; Zorn, J. A.; Gray, D. C.; Wells, J. A. *Science* **2009**, *326*, 853.
(29) Walsh, J. G.; Cullen, S. P.; Sheridan, C.; Lüthi, A. U.; Gerner, C.; Martin, S. J. *Proc. Natl. Acad. Sci. U.S.A.* **2008**, *105*, 12815.
(30) Shimbo, K.; Hsu, G. W.; Nguyen, H.; Mahrus, S.; Trinidad, J. C.; Burlingame, A. L.; Wells, J. A. *Proc. Natl. Acad. Sci. U.S.A.* **2012**, *109*, 12432.
(31) Burguillos, M. A.; Deierborg, T.; Kavanagh, E.; Persson, A.; Hajji, N.; Garcia-Quintanilla, A.; Cano, J.; Brundin, P.; Englund, E.; Venero, J. L.; Joseph, B. *Nature* **2011**, *472*, 319.

(32) Al-Jamala, K. T.; Gherardini, L.; Bardi, G.; Nunes, A.; Guo, C.; Bussy, C.; Herrero, M. A.; Bianco, A.; Prato, M.; Kostarelos, K.; Pizzorusso, T. *Proc. Natl. Acad. Sci. U.S.A.* **2011**, *108*, 10952.
(33) Porter, A. G.; Jänicke, R. U. *Cell Death Differ.* **1999**, *6*, 99.
(34) Gray, D. C.; Mahrus, S.; Wells, J. A. *Cell* **2010**, *142*, 637.
(35) Xiao, J.; Broz, P.; Puri, A. W.; Deu, E.; Morell, M.; Monack, D. M.; Bogyo, M. *J. Am. Chem. Soc.* **2013**, *135*, 9130.
(36) Edgington, L. E.; van Raam, B. J.; Verdoes, M.; Wierschem, C.; Salvesen, G. S.; Bogyo, M. *Chem. Biol.* **2012**, *19*, 340.
(37) Paulick, M. G.; Bogyo, M. *Curr. Opin. Genet. Dev.* **2008**, *18*, 97.
(38) Nomura, D. K.; Dix, M. M.; Cravatt, B. F. *Nat. Rev. Cancer* **2010**, *10*, 630, 638.
(39) Serim, S.; Haedke, U.; Verhelst, S. H. L. *ChemMedChem* **2012**, *7*, 1146.
(40) Kato, D.; Boatright, K. M.; Berger, A. B.; Nazif, T.; Blum, G.; Ryan, C.; Chehade, K. A.; Salvesen, G. S.; Bogyo, M. *Nat. Chem. Biol.* **2005**, *1*, 33.
(41) Edgington, L. E.; Verdoes, M.; Ortega, A.; Withana, N. P.; Lee, J.; Syed, S.; Bachmann, M. H.; Blum, G.; Bogyo, M. *J. Am. Chem. Soc.* **2013**, *135*, 174.
(42) Blum, G.; von Degenfeld, G.; Merchant, M. J.; Blau, H. M.; Bogyo, M. *Nat. Chem. Biol.* **2007**, *3*, 668.
(43) Berger, A. B.; Sexton, K. B.; Bogyo, M. *Cell Res.* **2006**, *16*, 961.
(44) Thornberry, N. A.; Rano, T. A.; Peterson, E. P.; Rasper, D. M.; Timkey, T.; Garcia-Calvo, M.; Houtzager, V. M.; Nordstrom, P. A.; Roy, S.; Vaillancourt, J. P.; Chapman, K. T.; Nicholson, D. W. *J. Biol. Chem.* **1997**, *272*, 17907.
(45) Denault, J. B. Salvesen, G. S. *Curr. Protoc. Protein Sci.* **2003**, Chapter 21:Unit 21.13.
(46) Vickers, C. J.; González-Páez, G. E.; Wolan, D. W. *ACS Chem. Biol.* **2013**, *8*, 1558.
(47) Pop, C.; Chen, Y. R.; Smith, B.; Bose, K.; Bobay, B.; Tripathy, A.; Franzen, S.; Clark, A. C. *Biochemistry* **2001**, *40*, 14224.
(48) Svingen, P. A.; Loegering, D.; Rodriquez, J.; Meng, X. W.; Mesner, P. W.; Holbeck, S.; Monks, A.; Krajewski, S.; Scudiero, D. A.; Sausville, E. A.; Reed, J. C.; Lazebnik, Y. A.; Kaufmann, S. H. *Clin. Cancer Res.* **2004**, *10*, 6807.
(49) Jänicke, R. U.; Sprengart, M. L.; Wati, M. R.; Porter, A. G. *J. Biol. Chem.* **1998**, *273*, 9357.
(50) Blanc, C.; Deveraux, Q. L.; Krajewski, S.; Jänicke, R. U.; Porter, A. G.; Reed, J. C.; Jaggi, R.; Marti, A. *Cancer Res.* **2000**, *60*, 4386.
(51) Voss, O. H.; Batra, S.; Kolattukudy, S. J.; Gonzalez-Mejia, M. E.; Smith, J. B.; Doseff, A. L. *J. Biol. Chem.* **2007**, *282*, 25088.
(52) Baliga, B. C.; Colussi, P. A.; Read, S. H.; Dias, M. M.; Jans, D. A.; Kumar, S. *J. Biol. Chem.* **2003**, *278*, 4899.
(53) Erener, S.; Pétrilli, V.; Kassner, I.; Minotti, R.; Castillo, R.; Santoro, R.; Hassa, P. O.; Tschopp, J.; Hottiger, M. O. *Mol. Cell* **2012**, *46*, 200.
(54) Kamada, S.; Kikkawa, U.; Tsujimoto, Y.; Hunter, T. *J. Biol. Chem.* **2005**, *280*, 857.
(55) Crawford, E. D.; Wells, J. A. *Annu. Rev. Biochem.* **2011**, *80*, 1055.
(56) Scott, C. W.; Sobotka-Briner, C.; Wilkins, D. E.; Jacobs, R. T.; Folmer, J. J.; Frazee, W. J.; Bhat, R. V.; Ghanekar, S. V.; Aharony, D. *J. Pharmacol. Exp. Ther.* **2003**, *304*, 433.
(57) Chauvier, D.; Ankri, S.; Charriaut-Marlangue, C.; Casimir, R.; Jacotot, E. *Cell Death Differ.* **2007**, *14*, 387.